



1 **Marine-Derived Water-Soluble Organic Nitrogen in**
2 **Coastal Air: Influence of Ocean Productivity on**
3 **Atmospheric Nitrogen Cycling**

4

5 Jiao Tang^{1,2}, Shujie Hu^{3*}; Xiao Wang⁴; Jiaqi Wang⁵, Shaojun Lv²; Xiaofei Geng²;
6 Guangcai Zhong², Yangzhi Mo², Surat Bualert⁶, Jun Li², Shizhen Zhao^{2*}; Gan
7 Zhang²

8

9 ¹ College of Marine Sciences, South China Agricultural University, Guangzhou
10 510642, China

11 ² State Key Laboratory of Advanced Environmental Technology, Guangzhou
12 Institute of Geochemistry, Chinese Academy of Sciences, Guangzhou, 510640,
13 China

14 ³ Chongqing Institute of Green and Intelligent Technology, Chinese Academy of
15 Sciences, Chongqing, 400714, China

16 ⁴ School of Resources and Environment, Henan Polytechnic University, Jiaozuo
17 454003, China

18 ⁵School of Electrical and Information Engineering, Zhengzhou University,
19 Zhengzhou, 450001, China

20 ⁶Faculty of Environment, Kasetsart University, Bangkok, 10900, Thailand

21

22 ***Correspondence to:** Shujie Hu (hushujie@cigit.ac.cn) and Shizhen Zhao
23 (zhaoshizhen@gig.ac.cn)

24



25 **Abstract**

26 Organic nitrogen (ON) deposition from aerosols plays a crucial role in
27 oceanic ecosystems; however, the influence of marine biogenic activity on
28 atmospheric ON remains poorly understood. Here, we investigate the
29 contribution of the marine biosphere to water-soluble organic nitrogen (WSON)
30 in coastal aerosols based on particulate matter samples collected in Bangkok,
31 Thailand, from January 2016 to January 2017. Concentrations of WSON and
32 water-soluble inorganic nitrogen (WSIN, including NO_3^- and NH_4^+) were
33 analyzed and compared across days classified by air mass origin over land as
34 marine-, mixed-, or continental-influenced. Air masses of marine origin showed
35 significantly lower WSON and WSIN concentrations than those from mixed and
36 continental origins. Nevertheless, the relative proportion of WSON in water-
37 soluble total nitrogen remained consistent, implying a persistent marine source.
38 Positive matrix factorization revealed that the contribution of sea spray aerosol
39 (SSA)-derived WSON increased markedly with oceanic influence, accounting
40 for $3.8\% \pm 6.4\%$, $14\% \pm 14\%$, and $34\% \pm 17\%$ under continental, mixed, and
41 marine conditions, respectively. Moreover, marine productivity, assessed via air
42 mass exposure to chlorophyll a concentrations (AEC), exhibited a strong
43 positive correlation with SSA-derived WSON ($r = 0.96$, $p < 0.001$), a finding
44 supported by large-scale reanalysis. These results provide direct evidence that
45 marine organic aerosols represent a major source of WSON in coastal regions
46 globally, with important implications for atmospheric nitrogen cycling and
47 climate feedback processes.

48

49



50 **1. Introduction**

51 Organic nitrogen (ON), which includes compounds such as amino acids,
52 urea, organic nitrates, nitroaromatics, and humic substances, plays an
53 important role in atmospheric processes including air quality, cloud formation,
54 and the nitrogen cycle (Cape *et al.*, 2011). On a global scale, water-soluble
55 organic nitrogen (WSON) has been estimated to contribute 10–40% of total
56 airborne ON (Matsumoto *et al.*, 2019a; Wang *et al.*, 2018), influencing aerosol
57 properties such as solubility, acidity, and hygroscopicity. Furthermore, certain
58 nitrogen-containing organic compounds, including nitroaromatics, have been
59 recognized as important chromophores in brown carbon (He *et al.*, 2022; Liu *et al.*,
60 *et al.*, 2023), thereby influencing radiative forcing. In addition, atmospheric
61 deposition of particulate WSON is increasingly regarded as a significant source
62 of nitrogen input to marine ecosystems (Buchanan *et al.*, 2021; Li *et al.*, 2023).

63 WSON originates from both direct emissions—including anthropogenic
64 and biogenic sources—and secondary formation through atmospheric
65 reactions (Xu *et al.*, 2020; Yu *et al.*, 2017). These complex sources and
66 atmospheric processes contribute to substantial spatial and temporal variability
67 in WSON deposition (Kanakidou *et al.*, 2012; Li *et al.*, 2023; Yu *et al.*, 2020).
68 Previous studies have identified marine emissions as a notable source of
69 atmospheric ON (Facchini *et al.*, 2008; O'Dowd *et al.*, 2004). Globally, the
70 estimated annual primary emission of soluble ON from the ocean is 2.1 Tg N
71 yr⁻¹, comparable in magnitude to anthropogenic emissions from fossil fuel
72 combustion and biomass burning (Ito *et al.*, 2014; Kanakidou *et al.*, 2012).
73 Consequently, organic nitrogen in marine aerosols is considered to be primarily
74 derived from biological production rather than terrestrial pollution (Altieri *et al.*,
75 2016).

76 Recent research has underscored the complexity and variability of WSON
77 in sea spray aerosol (SSA) (Altieri *et al.*, 2012; Li *et al.*, 2019). For instance,
78 primary emissions of sea salt particles have been recognized as a major source
79 of WSON over the remote Indian sector of the Southern Ocean (Matsumoto *et al.*,
80 *et al.*, 2022). These findings highlight the importance of incorporating marine ON
81 emissions in assessments of net atmospheric WSON deposition, particularly in
82 the open ocean (Luo *et al.*, 2018). However, several field studies in regions
83 strongly influenced by marine air masses have reported only minor
84 contributions from marine-derived WSON—typically below 5% (Leung *et al.*,



85 2024; Tsagkaraki *et al.*, 2021). This discrepancy indicates that distinguishing
86 anthropogenic from marine sources remains a challenge, even in coastal and
87 adjacent marine environments.

88 The Indochinese Peninsula (ICP), characterized by high population density
89 and substantial organic nitrogen (ON) deposition (Ito *et al.*, 2014; Kanakidou *et al.*,
90 2012; Li *et al.*, 2023), provides a suitable context for assessing the influence
91 of marine aerosols on atmospheric WSON. Eutrophication—the gradual
92 enrichment of aquatic ecosystems with nutrients such as nitrogen—enhances
93 primary productivity and can promote the subsequent emission of ON to the
94 atmosphere (Altieri *et al.*, 2016). Here, we selected Bangkok, the capital of
95 Thailand, which is situated in the central plain of the country and adjacent to
96 the Gulf of Thailand. The region experiences prevailing marine winds from
97 January to October, offering a favorable setting for studying marine aerosol
98 contributions to WSON. Our study aims to: (1) quantify WSON abundances at
99 a coastal site in the ICP; (2) assess marine influences on WSON distributions;
100 and (3) elucidate the mechanisms governing oceanic contributions to WSON.

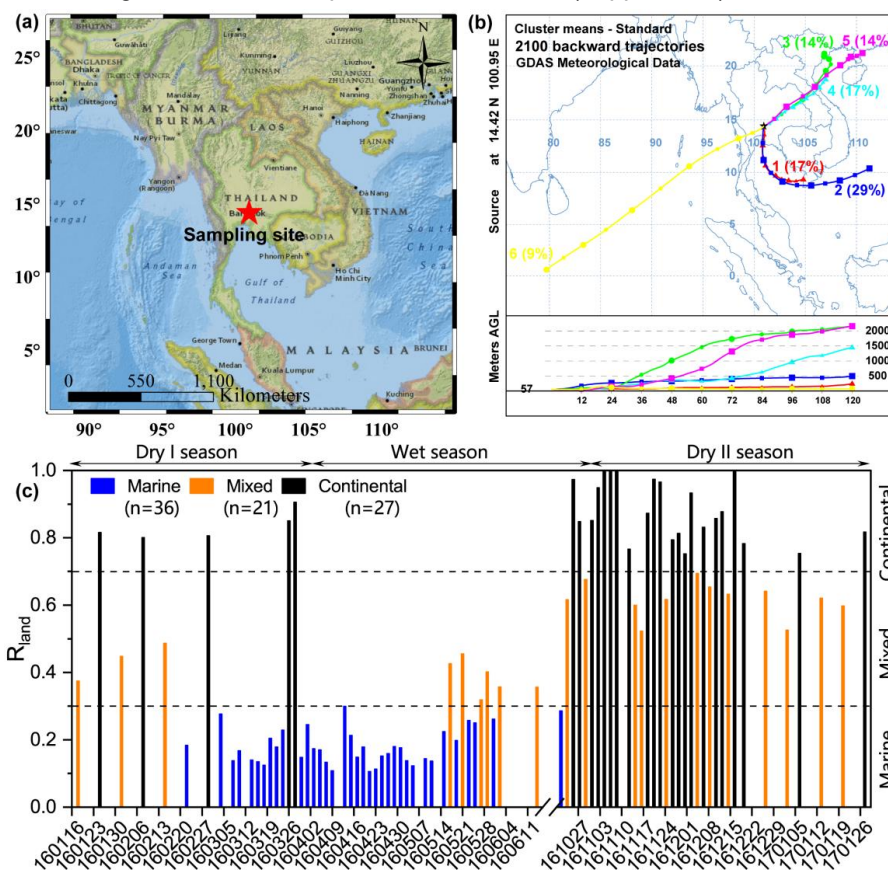
101 **2. Material and Methods**

102 **2.1. Sampling Campaign**

103 A total of 84 total suspended particulate (TSP) samples were collected from
104 the rooftop (57 m above ground level) of the Faculty of Environment at
105 Kasetsart University (100°57' E and 13°85' N; Figure 1a) in Bangkok,
106 Thailand—a site previously characterized in air quality studies (Tang *et al.*, 2021;
107 Wang *et al.*, 2020). Sampling was conducted over 24-hour periods using a high-
108 volume air sampler (flow rate: 0.3 m³ min⁻¹) equipped with pre-combusted
109 quartz-fiber filters (450 °C for 6 h). The collection period spanned from 18
110 January 2016 to 28 January 2017, covering three distinct seasons: Dry I
111 (January–March 2016), Wet (April–June and October 2016), and Dry II
112 (November 2016–January 2017). Sampling frequency averaged 5 ± 2 days per
113 month during January–February 2016 and January 2017, with intensified
114 campaigns in March–May and late October–December. Sampling was limited
115 between June and October due to heavy rainfall. Precipitation and solar
116 radiation data were obtained from historical reanalysis products provided by the
117 European Centre for Medium-Range Weather Forecasts (ECMWF). All
118 samples and field blanks were stored in the dark at –20 °C until analysis. A



119 summary of TSP mass concentrations, chemical components, and
120 meteorological conditions is provided in Table S1 (*Supplement*).



121
122 **Figure 1.** (a) Sampling site location in Bangkok, Thailand. (b) Classified air mass
123 trajectories (detailed in Figure S1–S2). (c) Distribution of the air mass retention ratio over
124 land (R_{land}), with samples categorized as marine-influenced ($R_{land} < 0.3$), mixed-influenced
125 ($0.3 \leq R_{land} \leq 0.7$), or continental-influenced ($R_{land} > 0.7$) based on the R_{land} values. The map
126 in panel (a) was created using ArcGIS software with the base layer from the ESRI National
127 Geographic World Map.

128 2.2. Chemical Analysis

129 Organic carbon (OC) and elemental carbon (EC) mass concentrations
130 were determined using an OC/EC analyzer following the NIOSH870 thermal-
131 optical protocol. Inorganic ions (Cl^- , NO_3^- , SO_4^{2-} , Na^+ , K^+ , NH_4^+ , Mg^{2+} , and Ca^{2+})
132 were quantified by ion chromatography (761 Compact IC, Metrohm,
133 Switzerland), and trace elements were analyzed via inductively coupled



134 plasma–mass spectrometry (ICP–MS; ELAN DRC II, PerkinElmer Ltd., Hong
135 Kong). Analytical errors were 5.5% for OC, and 3.9% for EC, below 5.0% for
136 trace element, and under 1.0% for water soluble ions , based on prior validation
137 (Wang *et al.*, 2020).

138 Polar molecular tracers—including biomass burning markers
139 (levoglucosan, mannosan, galactosan) and biogenic/anthropogenic secondary
140 organic aerosol tracers such as 2-methylglyceric acid (2-MGA), 2-methylthreitol
141 and 2-methylerythritol (2-MGL), 3-methyl-1,2,3-butanetricarboxylic acid
142 (MBTCA), and o/p-phthalic acid—were analyzed by gas chromatography–mass
143 spectrometry (GC–MS) following derivatization as previously reported (Geng *et al.*,
144 2020; Li *et al.*, 2013). The mean recovery of ¹³C-labeled levoglucosan was
145 87% ± 10%. Non-polar tracers of coal and fossil fuel combustion (hopanes and
146 steranes) were also analyzed, with perdeuterated tetracosane yielding a
147 recovery of 114% ± 11% (Wang *et al.*, 2020).

148 Water-soluble OC (WSOC) and water-soluble total nitrogen (WSTN) were
149 extracted by ultrasonication for 30 minutes using ultrapure water (resistivity >
150 18.2M·cm⁻¹), followed by filtration through 0.22 μm PTFE membranes.
151 Concentrations were measured with a total organic carbon/total nitrogen
152 analyzer (model TOC-Vcsh, Shimadzu). WSON was calculated as the
153 difference between WSTN and water-soluble inorganic nitrogen (WSIN), where
154 WSIN comprises NH₄⁺-N, NO₃⁻-N, NO₂⁻-N: [WSON] = [WSTN] – [WSIN]. Nitrite
155 concentrations were consistently below the detection limit of ion
156 chromatography and were excluded from further analysis. It should be noted
157 that some dissolved organic nitrogen species may not be fully converted to
158 nitrogen monoxide in the TOC/TN analyzer, potentially leading to
159 underestimation of WSON (Miyazaki *et al.*, 2011).

160 The relative standard deviation (RSD) for WSTN analysis were 3.6%
161 (method) and 0.77% (instrument). Method detection limits were 0.09 μg m⁻³ for
162 WSON, 0.03 μg m⁻³ for NO₃⁻, and 0.02 μg m⁻³ for NH₄⁺. Field blank levels were
163 0.067 μgN m⁻³ (WSON), 0.043 μgN m⁻³ (NH₄⁺-N), and 0.07 μgN m⁻³ (NO₃⁻-N),
164 corresponding to average blank-to-sample ratios of 7.1%, 4.3 %, and 12%,
165 respectively, consistent with previous reports (Matsumoto *et al.*, 2019a). All
166 reported WSON and WSTN concentrations were blank-corrected.



167 **2.3 Source Apportionment**

168 The U.S. Environmental Protection Agency's Positive Matrix Factorization
169 model (PMF 5.0) was employed to perform factor analysis on environmental
170 data with non-negativity constraints and to estimate associated uncertainties
171 (Norris *et al.*, 2014). PMF has been widely applied as a robust tool for aerosol
172 source apportionment. In PMF 5.0, species are evaluated based on the signal-
173 to-noise (S/N) ratio and can be classified as "strong," "weak," or "bad.". Weak
174 species are retained but assigned a tripled uncertainty, whereas bad species
175 are excluded from the modeling. In this study, WSON was included as a total
176 variable to resolve its sources. Following the base run, rotational stability (F_{peak})
177 tests were conducted, and model robustness was evaluated using the base
178 model displacement (DISP), bootstrap (BS), and bootstrap displacement (BS-
179 DISP) methods. A detailed description of PMF procedures is provided in Text
180 S1 in *Supplement*.

181 **2.4. Air Mass Back Trajectories and Trajectory-Based chlorophyll a.**

182 To identify potential source regions, we calculated 120-hour back
183 trajectories using the Hybrid Single-particle Lagrangian Integrated Trajectory
184 (HYSPLIT) model (<http://www.arl.noaa.gov/HYSPLIT.php>), driven by the Global
185 Data Assimilation System (GDAS) meteorological dataset at $1^\circ \times 1^\circ$ resolution
186 (<http://ready.arl.noaa.gov/archives.php>). Trajectories were generated at 1-hour
187 intervals and subsequently classified through cluster analysis (Figure 1b and
188 Figures S1–S2). Based on origin and transport pathways, air masses arriving
189 in Bangkok were grouped into six distinct clusters. During the Dry I season, air
190 masses originated predominantly over the Thailand Bay/South China Sea
191 (clusters 1–2), with a minor contribution from the Indochina Peninsula (cluster
192 3). In the Wet season, trajectories were primarily transported via the South
193 China Sea/Thailand Bay and the Arabian Sea (clusters 1, 2, 6), whereas Dry II
194 season air masses mainly originated over mainland China and crossed the
195 Indochina Peninsula (clusters 3–5).

196 Furthermore, the air mass retention ratio over land (R_{land}), defined as the
197 weighted ratio of transport time over land to the total transport duration, was
198 calculated according to the method of Zhou *et al.* (2021, 2023) using Equation
199 1. This parameter provides a quantitative measure of terrestrial influence at the
200 receptor site. A schematic illustration is presented in Figure S3.



201
$$R_{land} = \frac{\sum_{i=1}^{N_{land}} e^{-t_i/120}}{\sum_{i=1}^{N_{total}} e^{-t_i/120}} \quad (1)$$

202 Here, N_{total} denotes the total number of trajectory endpoints and N_{land}
203 the number over land. The backward tracking time t_i (in hours) and the
204 weighting factor $e^{-t_i/120}$ account for the diminishing influence of distant
205 regions due to air mass diffusion and particle deposition during transport. As a
206 result, regions associated with longer backward tracking times exert a weaker
207 influence on the receptor site compared to nearby areas. Based on the R_{land}
208 values (Figure 1c), samples were categorized as marine-influenced ($R_{land} < 0.3$),
209 mixed-influenced ($0.3 \leq R_{land} \leq 0.7$), or continental-influenced ($R_{land} > 0.7$). This
210 classification is further supported by molecular marker analysis: during marine-
211 influenced periods, the regression slope for Na^+ versus Mg^{2+} (0.11) closely
212 aligned with the seawater reference ratio (0.12). Elevated levels of Cl^- , Na^+ ,
213 non-sea-salt sulfate (nss-SO_4^{2-}), and $\text{Na}^+/\sum\text{ions}$ ratio consistently reflected
214 dominant contributions from sea spray emissions. Although long-range
215 anthropogenic transport may contribute to nss-SO_4^{2-} , marine biogenic sources
216 prevailed, with concentrations significantly higher during marine-influenced
217 periods than during mixed or continental periods. In contrast, combustion-
218 derived species such as non-sea-salt K^+ (nss-K^+), EC, and levoglucosan
219 showed markedly higher concentrations during continental- and mixed-
220 influenced periods than during marine-influenced periods (Table S2).

221 Air mass exposure to chlorophyll-a (AEC), defined as the mean sea
222 surface chlorophyll-a concentration along air mass trajectories, was used as a
223 proxy for marine biogenic emissions at the receptor site (Park *et al.*, 2018; Zhou
224 *et al.*, 2023). A statistically significant positive correlation was observed when
225 air masses traveled within the marine boundary layer. However, due to the
226 relatively low correlation between AEC and methanesulfonate, the formulation
227 was adjusted based on the approach of Zhou *et al.* (2021, 2023), as follows:

228
$$AEC = \frac{\sum_{i=1}^{N_{total}} Chla_i \cdot e^{-t_i/120} \cdot e^{-h_i/500}}{n} \quad (2)$$

229 Here, N_{total} denotes the total number of hourly endpoints (120, including
230 the receptor point) along the trajectory. The variable $Chla_i$ represents the
231 mean chlorophyll-a concentration—derived from MODIS-Aqua monthly
232 composites at a 4 km resolution—within a 20 km radius of the i_{th} trajectory



233 endpoint. Endpoints over land were assigned $Chla_i = \text{zero}$. The weighting
234 factor $e^{-h_i/500}$ accounts for the influence of altitude h_i , reflecting the reduced
235 contribution from higher altitudes due to chlorophyll dilution and particle
236 deposition during transport. The denominator n corresponds to the number of
237 trajectory endpoints with valid chlorophyll-a data, including zero values over
238 land.

239 **2.5. Potential Source Contribution Function (PSCF) Model**

240 The PSCF model was employed to identify source regions by discretizing
241 the study domain into an $i \times j$ grid. The PSCF values, ranging from 0 to 1,
242 represent the conditional probability that an air parcel passing through a grid
243 cell contributes to high concentrations at the receptor site; elevated values
244 denote a higher probability of source contribution. In this study, PSCF analysis
245 was applied to identify potential geographic source regions of both total WSON
246 and PMF-resolved source categories of WSON in aerosols collected in
247 Bangkok. A detailed description of the PSCF methodology is provided in Text
248 S2 and in previous publications (Geng *et al.*, 2020; Tang *et al.*, 2024).

249 **3. Results and Discussion**

250 **3.1. Temporal Variations of WSON**

251 Figure S4 and Table S1 present the temporal variations and statistical
252 summaries of meteorological parameters and chemical compositions in TSP
253 throughout the sampling campaign. In Bangkok, Thailand, the mass
254 concentrations of TSP, OC, and EC ranged from 17 to 161 $\mu\text{g m}^{-3}$ (mean: $55 \pm$
255 $30 \mu\text{g m}^{-3}$), 3.7 to 38 $\mu\text{g m}^{-3}$ (mean: $12 \pm 6.3 \mu\text{g m}^{-3}$), and 0.16 to 2.8 $\mu\text{g m}^{-3}$
256 (mean: $1.4 \pm 0.43 \mu\text{g m}^{-3}$), respectively. The TSP level in this region were
257 substantially lower than those reported in other areas, such as the Eastern
258 Mediterranean ($219.90 \pm 104.85 \mu\text{g m}^{-3}$; Tripathee *et al.*, 2021), Jiaozhou Bay
259 ($133.7 \pm 80.35 \mu\text{g m}^{-3}$; Xing *et al.*, 2018), and Xi'an during the dust episodes
260 ($2109 \pm 1360 \mu\text{g m}^{-3}$; Wang *et al.*, 2014). Pronounced seasonal variations were
261 observed: TSP levels decreased by 56% from the Dry I season to the Wet
262 season, but increased by 52% during the Dry II season. Rainfall during the Wet
263 season (April to October) accounted for 92% of the annual precipitation total.
264 To examine wet scavenging effects, we evaluated the relationship between TSP
265 concentrations and precipitation (Figure S5a). A significant negative correlation
266 was identified ($R^2 = 0.22$, $p < 0.001$), indicating efficient aerosol removal by



267 rainfall. The relatively low R^2 value, however, suggests additional influences
268 from emission sources and precipitation occurring during long-range transport.

269 The mass fraction of WSTN in TSP collected in Bangkok averaged $3.8\% \pm$
270 1.1% (range $2.2\%–7.2\%$), higher than that reported in the Eastern
271 Mediterranean ($\sim 2.7\%$; Tripathee *et al.*, 2021) and comparable to values from
272 Sapporo, Japan ($3.81\% \pm 2.28\%$; Pavuluri *et al.*, 2015), underscoring the
273 relevance of water-soluble nitrogen in this region. As shown in Figure 2a and
274 Table S2, concentrations of WSON, NO_3^- -N, and NH_4^+ -N ranged from $0.27–2.3$
275 $\mu\text{gN m}^{-3}$ ($0.95 \pm 0.40 \mu\text{gN m}^{-3}$), below detection limitation (BDL)– $2.7 \mu\text{gN m}^{-3}$
276 ($0.60 \pm 0.52 \mu\text{gN m}^{-3}$), and BDL– $2.2 \mu\text{gN m}^{-3}$ ($0.47 \pm 0.44 \mu\text{gN m}^{-3}$),
277 respectively. WSON correlated positively with both TSP ($r = 0.65$, $p < 0.01$) and
278 WSIN ($r = 0.51$, $p < 0.01$), suggesting possible common sources or formation
279 pathways (Figure S6).

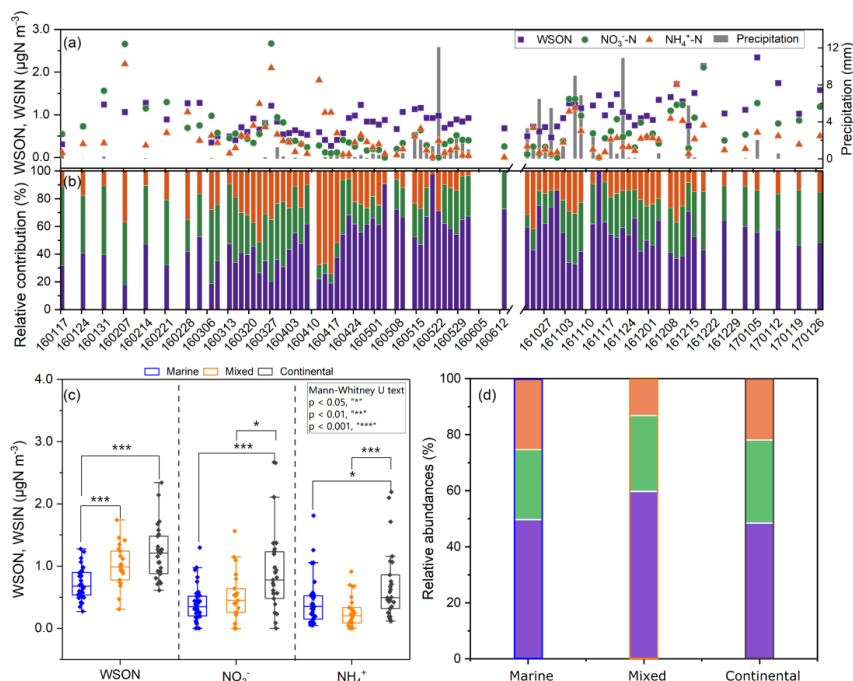
280 Concentrations of WSON, NO_3^- -N, NH_4^+ -N, TSP, OC, and EC varied
281 considerably under different air mass regimes (Table S2). The nonparametric
282 Mann–Whitney U test indicated that WSON and NO_3^- -N levels were
283 significantly lower during marine-influenced periods than under mixed or
284 continental conditions (Figure 2c, $p < 0.001$). In contrast, NH_4^+ -N concentrations
285 were slightly elevated during marine periods, consistent with the ocean
286 potentially acting as a source of atmospheric ammonia (Altieri *et al.*, 2014). This
287 pattern aligns with earlier studies reporting higher WSON in aerosols of remote
288 marine regions under continental influence than in those of purely oceanic
289 origin, indicating a stronger terrestrial contribution (Jickells *et al.*, 2013).
290 Biomass burning tracers (e.g., levoglucosan, galactosan, mannosan) were also
291 significantly lower during marine-influenced days (see Table S2). Furthermore,
292 WSON correlated with biomass burning markers and SOA markers and aerosol
293 liquid water content (ALWC, Text S3) under mixed and continental conditions—
294 associations absent during marine periods (Figure S7). Wet scavenging may
295 partly explain the lower WSON levels in marine periods, which largely coincided
296 with the rainy season (Figure 2a), though no direct correlation was found
297 between WSON and precipitation (Figure S5b).

298 The WSON/WSTN ratio during marine-influenced days ($50\% \pm 17\%$) was
299 similar to that under continental influence ($48\% \pm 15\%$) but lower than during
300 mixed conditions ($60\% \pm 17\%$) (Figure 2d). Continental WSON/WSTN ratios
301 likely reflect anthropogenic emissions, whereas marine periods may be



302 influenced by marine biogenic emissions or shipping activity from Bangkok Port.
303 Mixed conditions likely represent combined source influences. Precipitation
304 may alter the WSON/WSTN ratio through differential scavenging: WSIN
305 species (e.g., nitrate, ammonium) are efficiently removed by rainfall
306 (Matsumoto *et al.*, 2019b; Nehir and Koçak, 2018), as shown by their strong
307 correlation with precipitation (Figure S5c,d), whereas the lack of such a
308 correlation for WSON suggests distinct scavenging behavior.

309 Annually, WSON accounted for $52\% \pm 17\%$ of the WSTN (Figure 2b)—
310 substantially higher than values reported from a forest site ($20\% \pm 11\%$;
311 Miyazaki *et al.*, 2014), an offshore island (27%; Tian *et al.*, 2023), Sapporo (9.2%
312 $\pm 7.3\%$; Pavuluri *et al.*, 2015), and coastal Qingdao ($\sim 20\%$; Shi *et al.*, 2010).
313 Elevated WSON/WSTN ratios have been documented in source emissions
314 such as biomass burning ($80\% \pm 6.3\%$), vehicle exhaust ($67\% \pm 16\%$), and ship
315 emissions ($54\% \pm 31\%$) (Yu *et al.*, 2017), as well as in polluted continental
316 regions like Hawaii (64%; Cornell *et al.*, 2001) and Xi'an (45%, range: 22–68%;
317 Ho *et al.*, 2015). By comparison, the South China Sea—characterized by
318 marine background conditions—exhibited a WSON/WSTN ratio of 34%, higher
319 than that of the Yellow Sea (17%; Shi *et al.*, 2010). During phytoplankton
320 blooms, organic nitrogen can dominate aerosol composition, contributing up to
321 84% of total dissolved nitrogen (Violaki *et al.*, 2015) and 63% of submicrometer
322 aerosol mass (O'Dowd *et al.*, 2004). Collectively, these studies indicate that
323 elevated WSON/WSTN ratios may arise from either anthropogenic influence or
324 marine biogenic activity. Therefore, the WSON/WSTN ratio alone is insufficient
325 to discriminate marine and anthropogenic sources of WSON. More quantitative
326 approaches are needed to apportion the origins of aerosol organic nitrogen.
327



328

329 **Figure 2.** Temporal variations and source influences on nitrogen species in Bangkok
330 aerosols. (a) Time-series of concentrations of WSON and WSIN (NH_4^+ -N, NO_3^- -N),
331 overlaid with daily rainfall from ECMWF reanalysis data. (b) Relative contributions of
332 WSON and WSIN to total water-soluble nitrogen across the study period. (c) Concentration
333 distributions and (d) relative abundances of WSON and WSIN during marine-, mixed-, and
334 continental-influenced periods.

335 3.2. Sea Spray Aerosols as a Major WSON Source in Marine- 336 influenced Days

337 To elucidate the contributions of marine and anthropogenic sources to
338 WSON in this coastal urban environment, we applied the PMF 5.0 model to 84
339 aerosol samples characterized by 26 chemical species. The model resolved
340 WSON into seven source factors: ship emissions, secondary sulfate, dust,
341 secondary organic aerosol (SOA), biomass burning (BB), vehicle emissions
342 and fossil combustion (VEFC), and sea spray aerosol (SSA) (Figure S8). Here,
343 the SSA factor was identified by high loadings of Na^+ , Cl^- , and Mg, because we
344 note that SSA-derived WSON was significantly associated with marine
345 biological activity—not merely sea-salt particles—as elaborated below.



346 Furthermore, PSCF mapping of SSA-derived WSON was mainly associated
347 with the Gulf of Thailand and, to a lesser extent, the Bay of Bengal, reinforcing
348 the role of sea spray as a relevant WSON source.

349 Over the entire study period, SOA ($34\% \pm 25\%$), VEFC ($21\% \pm 16\%$), SSA
350 ($19\% \pm 19\%$), and BB ($13\% \pm 12\%$) emerged as the dominant sources of WSON
351 in Bangkok aerosols (Figures 3b and S9). This is consistent with previous
352 reports highlighting secondary formation and biomass burning as major
353 contributors to WSON (Leung *et al.*, 2024; Tsagkaraki *et al.*, 2021; Yu *et al.*,
354 2017). Earlier factor-based studies also indicated that sea salt can explain over
355 20% of the variance in WSON (Chen and Chen, 2010; Shi *et al.*, 2010). The
356 contribution of SSA in our study, however, exceeded values reported for other
357 coastal regions such as Hong Kong (4.4%) and the Eastern Mediterranean
358 ($<5\%$) (Leung *et al.*, 2024; Nehir and Koçak, 2018; Tsagkaraki *et al.*, 2021). Two
359 factors may explain this discrepancy. First, organic nitrogen in coarse aerosols
360 often originates from soil, dust, or large sea-salt particles (Cornell *et al.*, 2001;
361 Mace *et al.*, 2003), whereas studies focusing on $PM_{2.5}$ —such as those in Hong
362 Kong—naturally record lower sea-salt contributions (Leung *et al.*, 2024).
363 Second, the ultra-oligotrophic marine environment of the Eastern
364 Mediterranean, characterized by low nutrient availability and limited riverine
365 input, results in low marine productivity and thus diminished marine-derived
366 WSON (Nehir and Koçak, 2018; Tsagkaraki *et al.*, 2021).

367 We further disaggregated WSON source contributions by air mass regime
368 Figure 3b. Under marine influence, SSA constituted the dominant source of
369 WSON ($34\% \pm 17\%$), exceeding SOA ($19\% \pm 17\%$) and VEFC ($19\% \pm 14\%$),
370 while BB contributed minimally ($7.1\% \pm 6.0\%$). This pattern is consistent with
371 studies conducted in remote marine and island settings (Altieri *et al.*, 2016;
372 Miyazaki *et al.*, 2011; Violaki *et al.*, 2015). Under mixed marine–continental
373 influence, SOA became the dominant contributor ($51\% \pm 20\%$), followed by
374 VEFC ($19\% \pm 14\%$) and SSA ($14\% \pm 15\%$). During continental conditions, SOA
375 remained the primary source ($41\% \pm 26\%$), likely due to the formation of
376 nitroaromatic compounds from biogenic and anthropogenic volatile organic
377 compounds under NO_x and H_2O_2 exposure (Xie *et al.*, 2017). Previous work
378 has shown that oxidized α -pinene SOA can account for 33%–37.7% of WSON,
379 with aerosol liquid water further promoting nighttime secondary WSON
380 formation (Xu *et al.*, 2020). Under continental regimes, VEFC ($26\% \pm 19\%$) and

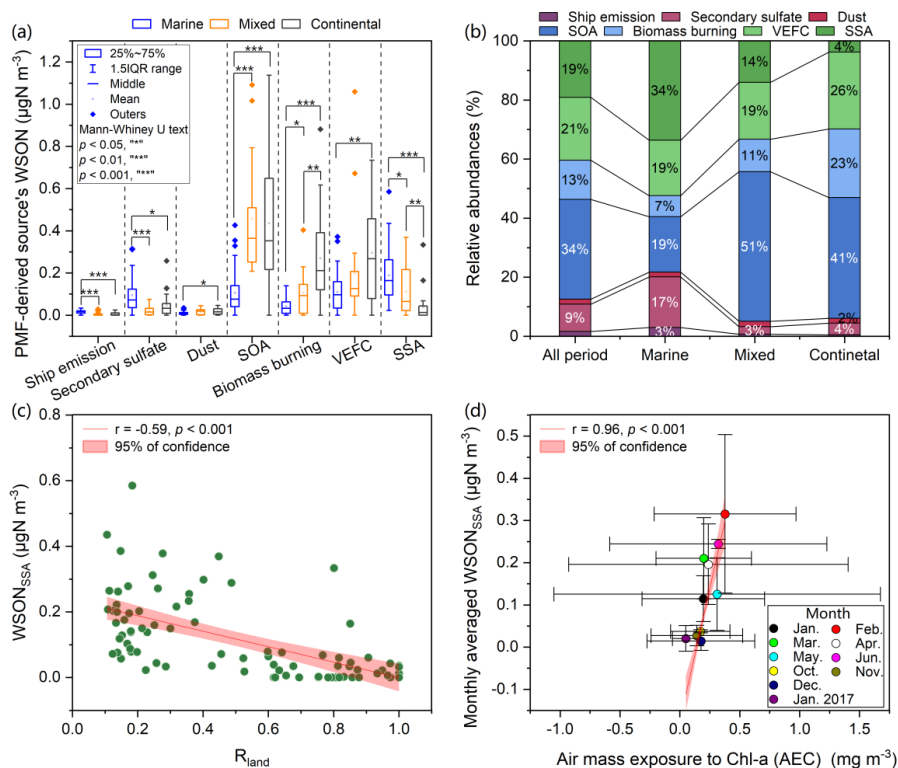


381 BB ($23\% \pm 14\%$) also contributed substantially to WSON. Notably, the SSA
382 contribution dropped sharply to $3.8\% \pm 6.4\%$ under continental influence.

383 Temporal variations in source-resolved WSON concentrations are shown
384 in Figure 3a. Among the three air mass regimes, SSA-derived WSON
385 concentrations peaked under marine influence ($0.19 \pm 0.12 \mu\text{gN m}^{-3}$),
386 approximately 1.7 times higher than during mixed periods ($0.11 \pm 0.12 \mu\text{gN m}^{-3}$)
387 and five times higher than during continental periods ($0.037 \pm 0.069 \mu\text{gN m}^{-3}$).
388 Ship-emission-derived WSON was also elevated during marine days (0.015
389 $\pm 0.0075 \mu\text{gN m}^{-3}$) relative to mixed and continental periods, though its overall
390 contribution remained low ($\sim 3\%$). These results underscore marine air mass
391 transport as the principal driver of SSA-derived WSON, further supported by a
392 strong negative correlation between SSA-WSON and R_{land} (Figure 3c, $r = -0.59$,
393 $p < 0.001$). In contrast, SOA-, BB-, and VEFC-derived WSON increased
394 significantly under mixed and continental conditions. Although SOA is generally
395 considered more susceptible to wet removal than primary aerosol (Sun *et al.*,
396 2011; Zhao *et al.*, 2026), no correlation was observed between precipitation and
397 PMF-resolved source contributions, suggesting limited wet scavenging
398 influence on WSON composition.

399

400



401

402 **Figure 3.** Source apportionment of WSON based on PMF. (a) Absolute concentrations and
 403 (b) relative contributions of PMF-resolved sources to total WSON during the entire study
 404 period and under marine-, mixed-, and continental-influenced conditions. (c) Correlation
 405 between R_{land} and SSA-derived WSON. (d) Relationship between air mass exposure to
 406 chlorophyll-a (AEC) and monthly averaged SSA-derived WSON concentrations, color-
 407 coded by sampling month.

408 **3.3. Marine Productivity as a Key Factor influenced coastal WSON**
 409 **Distribution**

410 SSA comprises a complex mixture of organic compounds derived from the
 411 ocean surface (Prather *et al.*, 2013; Quinn *et al.*, 2014; Schiffer *et al.*, 2018).
 412 Numerous studies have identified marine biological productivity as a major
 413 source of WSON in remote marine regions (O'Dowd *et al.*, 2015; Violaki *et al.*,
 414 2015). Satellite-derived chlorophyll-a (Chl-a) concentrations, which provide
 415 global coverage of oceanic phytoplankton biomass, are widely used as a proxy
 416 for the organic fraction in SSA (Facchini *et al.*, 2008; O'Dowd *et al.*, 2004).



417 Consistent with this, ON and OC concentrations in marine aerosols from highly
418 productive waters are approximately twice those from oligotrophic regions
419 (Miyazaki *et al.*, 2010). Stable carbon isotope analyses further indicate that
420 marine-derived carbon can contribute 46%–72% of total aerosol carbon in
421 productive oceanic areas (Miyazaki *et al.*, 2010). A seasonal pattern linking both
422 Chl-a and water-insoluble OC has been documented (O'Dowd *et al.*, 2008).
423 Given the substantial contribution of SSA to WSON during marine-influenced
424 periods in our study, we investigated marine productivity as a key driver of
425 WSON distribution.

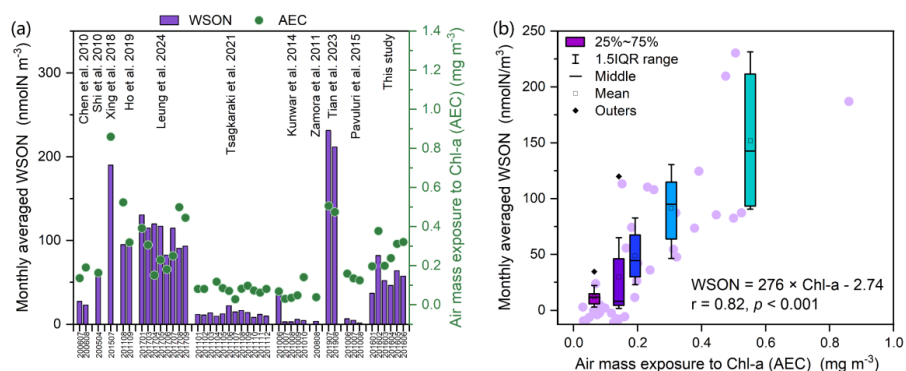
426 We calculated air mass exposure to chlorophyll-a (AEC) based on monthly
427 MODIS Chl-a data (4 km resolution) along 120-hour backward trajectories (see
428 Methods). SSA-derived WSON exhibited a strong positive correlation with AEC
429 ($r = 0.96$, $p < 0.001$; Figure 3d), highlighting phytoplankton's role in aerosol
430 composition. This contrasts with Tian *et al.* (2023), who observed significant
431 WSON-AEC correlations only in summer, likely due to dominant anthropogenic
432 influences suppressing marine signatures during other seasons. While previous
433 multivariate regression identified wind speed and Chl-a as key predictors of the
434 organic fraction in SSA (Gantt *et al.*, 2011), other studies note that Chl-a alone
435 may not fully capture organic enrichment (Rinaldi *et al.*, 2013). Nevertheless,
436 moderate correlations ($r \approx 0.60$) between Chl-a and marine organic aerosol
437 abundance have been reported (Sciare *et al.*, 2009). Collectively, these findings
438 indicate that biogenic organic matter—enriched in lipids, proteins, and humic
439 substances in the sea surface microlayer and transferred via bubble bursting—
440 is a primary source of WSON in Bangkok during marine air mass influence.

441 To better understand the large-scale role of oceanic WSON sources in
442 coastal regions affected by marine air masses, we compiled and analyzed a
443 global dataset of WSON concentrations from coastal and island sites. We
444 consistently applied HYSPLIT trajectory analysis, R_{land} calculation, and AEC
445 estimation based on MODIS Chl-a to all sites (Figure 4a and Table S3). Spatially,
446 the highest WSON concentrations occurred at Huaniao Island (Tian *et al.*, 2023),
447 followed by Jiaozhou Bay (Xing *et al.*, 2018), Hong Kong (Ho *et al.*, 2019; Leung
448 *et al.*, 2024), the South China Sea (Shi *et al.*, 2010), and Bangkok. The lowest
449 values were observed in the Eastern Mediterranean (Tsagkaraki *et al.*, 2021),
450 Keelung City (Chen and Chen, 2010), Okinawa Island (Kunwar and Kawamura,
451 2014), Barbados (Zamora *et al.*, 2011), and Sapporo (Pavuluri *et al.*, 2015).



452 Notably, spatial patterns in AEC closely mirrored those in WSON. A significant
453 positive correlation was found between WSON and AEC across all sites ($r =$
454 0.82 , $WSON [nmol m^{-3}] = 276 \times AEC [mg m^{-3}] - 2.74$, Figure 4b), that WSON
455 levels in marine-influenced coastal aerosols are strongly linked to ocean
456 surface productivity along the air mass transport pathway.

457



458

459 **Figure 4.** (a) Geographic distributions and (b) correlation between monthly mean air mass
460 exposure to Chl-a (AEC) concentrations and monthly mean WSON concentration in
461 coastal regions predominantly influenced by marine air masses. Values are provided in
462 Table S3. Air mass trajectories for these coastal and island sampling sites were
463 recalculated using the HYSPLIT model, and AEC values were derived from MODIS
464 monthly Chl-a concentrations.

465

4. Conclusions

466 The relationship derived in this study ($WSON [nmol m^{-3}] = 276 \times AEC [mg$
467 $m^{-3}] - 2.74$) provides a quantitative means to link marine aerosol composition
468 with oceanic biological activity. In the context of rising sea surface temperatures,
469 enhanced microalgal growth may elevate emissions of marine primary organic
470 aerosol, thereby introducing an important component into the aerosol–cloud–
471 climate feedback system. These findings highlight the necessity of
472 incorporating marine-derived organic nitrogen into climate models to better
473 represent interactions between marine ecosystems, atmospheric chemistry,
474 and climate regulation. Variations in marine productivity—whether natural or
475 anthropogenically driven—can directly modulate atmospheric nitrogen levels,
476 which may in turn influence oceanic nitrogen deposition and primary
477 productivity. Given that organic nitrogen deposition may also stimulate CO₂



478 uptake, this study underscores the role of marine ecosystems in climate
479 mitigation and calls for a more integrated understanding of global climate
480 dynamics.

481 Our results reveal a previously underestimated source of atmospheric
482 WSON derived from marine biota, particularly during periods of marine air mass
483 influence. The strong correlation between WSON and chlorophyll-a-based AEC
484 offers new evidence for the role of marine productivity in shaping atmospheric
485 nitrogen composition. In contrast to earlier studies that have largely overlooked
486 this pathway, our analysis identifies marine-derived organic nitrogen as a
487 relevant contributor, especially in productive coastal regions. This omission in
488 current climate models may lead to incomplete representations of nitrogen
489 cycling and aerosol processes. We therefore propose the integration of
490 satellite-derived chlorophyll-a data into air mass trajectory analyses, coupled
491 with the empirical relationship presented here, to better quantify marine-
492 sourced WSON. Integrating this component into climate models will refine
493 predictions of nitrogen deposition, ecosystem responses, and atmospheric
494 composition.

495 **Code and data availability.**

496 Data are available from the link (<https://doi.org/10.17605/OSF.IO/YMJ3F>).

497 **Supplement**

498 The supplement related to this article is available online.

499 **Author contributions**

500 Conceptualization: JT. Funding acquisition: JT, SH, SZ, and GZ.
501 Investigation: JT, XW, JW, SL, XG, GuZ, and SB. Methodology: JT, XW,
502 and JW. Project administration: GZ and SZ. Resources: YM, SZ, JL, and
503 GZ. Software: XW, and SL. Supervision: JL, SZ, and GZ. Validation: JT and
504 SZ. Writing (original draft): JT. Writing (review and editing): XW, SH, SZ,
505 and GZ.

506 **Notes**

507 The authors declare no competing financial interest.

508 **Acknowledgments**

509 This research has been supported by the National Natural Science
510 Foundation of China (42030715, 42192511, and 42207308), the Alliance of



511 International Science Organizations (ANSO-CR-KP-2021-05), the Guangdong
512 Basic and Applied Basic Research Foundation (2021A0505020017 and
513 2023B1515020067), the National Science Foundation of Chongqing
514 (CSTB2024NSCQ-MSX0897), and the Postdoctoral Fellowship Program of
515 CPSF (GZC20232684).

516 **References**

- 517 Altieri, K. E., S. E. Fawcett, A. J. Peters, D. M. Sigman, and M. G. Hastings (2016), Marine
518 biogenic source of atmospheric organic nitrogen in the subtropical North Atlantic, *Proc.*
519 *Natl. Acad. Sci. U. S. A.*, *113*(4), 925-930. <https://doi.org/10.1073/pnas.1516847113>.
- 520 Altieri, K. E., M. G. Hastings, A. J. Peters, S. Oleynik, and D. M. Sigman (2014), Isotopic
521 evidence for a marine ammonium source in rainwater at Bermuda, *Global Biogeochem.*
522 *Cycles*, *28*(10), 1066-1080. <https://doi.org/10.1002/2014GB004809>.
- 523 Altieri, K. E., M. G. Hastings, A. J. Peters, and D. M. Sigman (2012), Molecular
524 characterization of water soluble organic nitrogen in marine rainwater by ultra-high
525 resolution electrospray ionization mass spectrometry, *Atmos. Chem. Phys.*, *12*(7), 3557-
526 3571. <https://doi.org/10.5194/acp-12-3557-2012>.
- 527 Buchanan, P. J., O. Aumont, L. Bopp, C. Mahaffey, and A. Tagliabue (2021), Impact of
528 intensifying nitrogen limitation on ocean net primary production is fingerprinted by
529 nitrogen isotopes, *Nat. Commun.*, *12*(1), 6214. <https://doi.org/10.1038/s41467-021-26552-w>.
- 531 Cape, J. N., S. E. Cornell, T. D. Jickells, and E. Nemitz (2011), Organic nitrogen in the
532 atmosphere — Where does it come from? A review of sources and methods, *Atmos.*
533 *Res.*, *102*(1), 30-48. <https://doi.org/10.1016/j.atmosres.2011.07.009>.
- 534 Chen, H.-Y., and L.-D. Chen (2010), Occurrence of water soluble organic nitrogen in
535 aerosols at a coastal area, *J. Atmos. Chem.*, *65*(1), 49-71.
536 <https://doi.org/10.1007/s10874-010-9181-y>.
- 537 Cornell, S., K. Mace, S. Coeppicus, R. Duce, B. Huebert, T. Jickells, and L. Z. Zhuang
538 (2001), Organic nitrogen in Hawaiian rain and aerosol, *J. Geophys. Res.-Atmos.*,
539 *106*(D8), 7973-7983. <https://doi.org/10.1029/2000jd900655>.
- 540 Facchini, M. C., et al. (2008), Important Source of Marine Secondary Organic Aerosol from
541 Biogenic Amines, *Environ. Sci. Technol.*, *42*(24), 9116-9121.
542 <https://doi.org/10.1021/es8018385>.
- 543 Gantt, B., N. Meskhidze, M. C. Facchini, M. Rinaldi, D. Ceburnis, and C. D. O'Dowd (2011),
544 Wind speed dependent size-resolved parameterization for the organic mass fraction of
545 sea spray aerosol, *Atmos. Chem. Phys.*, *11*(16), 8777-8790. <https://doi.org/10.5194/acp-11-8777-2011>.
- 547 Geng, X., Y. Mo, J. Li, G. Zhong, J. Tang, H. Jiang, X. Ding, R. N. Malik, and G. Zhang
548 (2020), Source apportionment of water-soluble brown carbon in aerosols over the
549 northern South China Sea: Influence from land outflow, SOA formation and marine
550 emission, *Atmos. Environ.*, *229*, 117484.



- 551 <https://doi.org/10.1016/j.atmosenv.2020.117484>.
- 552 He, Q., C. Li, K. Siemens, A. C. Morales, A. P. S. Hettiyadura, A. Laskin, and Y. Rudich
553 (2022), Optical Properties of Secondary Organic Aerosol Produced by Photooxidation of
554 Naphthalene under NO_x Condition, *Environ. Sci. Technol.*, *56*(8), 4816-4827.
555 <https://doi.org/10.1021/acs.est.1c07328>.
- 556 Ho, K. F., S. S. H. Ho, R.-J. Huang, S. X. Liu, J.-J. Cao, T. Zhang, H.-C. Chuang, C. S.
557 Chan, D. Hu, and L. Tian (2015), Characteristics of water-soluble organic nitrogen in fine
558 particulate matter in the continental area of China, *Atmos. Environ.*, *106*, 252-261.
559 <https://doi.org/10.1016/j.atmosenv.2015.02.010>.
- 560 Ho, S. S. H., L. Li, L. Qu, J. Cao, K. H. Lui, X. Niu, S.-C. Lee, and K. F. Ho (2019), Seasonal
561 behavior of water-soluble organic nitrogen in fine particulate matter (PM_{2.5}) at urban
562 coastal environments in Hong Kong, *Air Qual. Atmos. Health*, *12*(4), 389-399.
563 <https://doi.org/10.1007/s11869-018-0654-5>.
- 564 Ito, A., G. Lin, and J. E. Penner (2014), Reconciling modeled and observed atmospheric
565 deposition of soluble organic nitrogen at coastal locations, *Global Biogeochem. Cycles*,
566 *28*(6), 617-630. <https://doi.org/10.1002/2013GB004721>.
- 567 Jickells, T., A. R. Baker, J. N. Cape, S. E. Cornell, and E. Nemitz (2013), The cycling of
568 organic nitrogen through the atmosphere, *Philosophical Transactions of the Royal
569 Society B: Biological Sciences*, *368*(1621), 20130115.
570 <https://doi.org/10.1098/rstb.2013.0115>.
- 571 Kanakidou, M., et al. (2012), Atmospheric fluxes of organic N and P to the global ocean,
572 *Global Biogeochem. Cycles*, *26*. <https://doi.org/10.1029/2011gb004277>.
- 573 Kunwar, B., and K. Kawamura (2014), One-year observations of carbonaceous and
574 nitrogenous components and major ions in the aerosols from subtropical Okinawa Island,
575 an outflow region of Asian dusts, *Atmos. Chem. Phys.*, *14*(4), 1819-1836.
576 <https://doi.org/10.5194/acp-14-1819-2014>.
- 577 Leung, C. W., X. Wang, and D. Hu (2024), Characteristics and source apportionment of
578 water-soluble organic nitrogen (WSON) in PM_{2.5} in Hong Kong: With focus on amines,
579 urea, and nitroaromatic compounds, *J. Hazard. Mater.*, *469*, 133899.
580 <https://doi.org/10.1016/j.jhazmat.2024.133899>.
- 581 Li, J. J., G. H. Wang, J. J. Cao, X. M. Wang, and R. J. Zhang (2013), Observation of
582 biogenic secondary organic aerosols in the atmosphere of a mountain site in central
583 China: temperature and relative humidity effects, *Atmos. Chem. Phys.*, *13*(22), 11535-
584 11549. <https://doi.org/10.5194/acp-13-11535-2013>.
- 585 Li, R., L. Cui, Y. Zhao, H. Fu, Q. Li, L. Zhang, and J. Chen (2019), Size-segregated water-
586 soluble N-bearing species in the land-sea boundary zone of East China, *Atmos. Environ.*,
587 *218*, 116990. <https://doi.org/10.1016/j.atmosenv.2019.116990>.
- 588 Li, Y., et al. (2023), Dissecting the contributions of organic nitrogen aerosols to global
589 atmospheric nitrogen deposition and implications for ecosystems, *Natl. Sci. Rev.*, *10*(12).
590 <https://doi.org/10.1093/nsr/nwad244>.
- 591 Liu, X., et al. (2023), Secondary Formation of Atmospheric Brown Carbon in China Haze:
592 Implication for an Enhancing Role of Ammonia, *Environ. Sci. Technol.*, *57*(30), 11163-



- 593 11172. <https://doi.org/10.1021/acs.est.3c03948>.
- 594 Luo, L., S. J. Kao, H. Bao, H. Xiao, H. Xiao, X. Yao, H. Gao, J. Li, and Y. Lu (2018), Sources
595 of reactive nitrogen in marine aerosol over the Northwest Pacific Ocean in spring, *Atmos.*
596 *Chem. Phys.*, *18*(9), 6207-6222. <https://doi.org/10.5194/acp-18-6207-2018>.
- 597 Mace, K. A., R. A. Duce, and N. W. Tindale (2003), Organic nitrogen in rain and aerosol at
598 Cape Grim, Tasmania, Australia, *J. Geophys. Res.-Atmos.*, *108*(D11).
599 <https://doi.org/10.1029/2002JD003051>.
- 600 Matsumoto, K., H. Kobayashi, K. Hara, S. Ishino, and M. Hayashi (2022), Water-soluble
601 organic nitrogen in fine aerosols over the Southern Ocean, *Atmos. Environ.*, *287*.
602 <https://doi.org/10.1016/j.atmosenv.2022.119287>.
- 603 Matsumoto, K., K. Sakata, and Y. Watanabe (2019a), Water-soluble and water-insoluble
604 organic nitrogen in the dry and wet deposition, *Atmos. Environ.*, *218*.
605 <https://doi.org/10.1016/j.atmosenv.2019.117022>.
- 606 Matsumoto, K., Y. Watanabe, K. Horiuchi, and T. Nakano (2019b), Simultaneous
607 measurement of the water-soluble organic nitrogen in the gas phase and aerosols at a
608 forested site in Japan, *Atmos. Environ.*, *200*, 312-318.
609 <https://doi.org/10.1016/j.atmosenv.2018.12.011>.
- 610 Miyazaki, Y., P. Fu, K. Ono, E. Tachibana, and K. Kawamura (2014), Seasonal cycles of
611 water-soluble organic nitrogen aerosols in a deciduous broadleaf forest in northern
612 Japan, *J. Geophys. Res.-Atmos.*, *119*(3), 1440-1454.
613 <https://doi.org/10.1002/2013jd020713>.
- 614 Miyazaki, Y., K. Kawamura, J. Jung, H. Furutani, and M. Uematsu (2011), Latitudinal
615 distributions of organic nitrogen and organic carbon in marine aerosols over the western
616 North Pacific, *Atmos. Chem. Phys.*, *11*(7), 3037-3049. <https://doi.org/10.5194/acp-11-3037-2011>.
- 617
- 618 Miyazaki, Y., K. Kawamura, and M. Sawano (2010), Size distributions of organic nitrogen
619 and carbon in remote marine aerosols: Evidence of marine biological origin based on
620 their isotopic ratios, *Geophys. Res. Lett.*, *37*(6). <https://doi.org/10.1029/2010GL042483>.
- 621 Nehir, M., and M. Koçak (2018), Atmospheric water-soluble organic nitrogen (WSON) in
622 the eastern Mediterranean: origin and ramifications regarding marine productivity, *Atmos.*
623 *Chem. Phys.*, *18*(5), 3603-3618. <https://doi.org/10.5194/acp-18-3603-2018>.
- 624 Norris, G., R. Duvall, S. Brown, and S. Bai (2014), EPA Positive Matrix Factorization (PMF)
625 5.0 fundamentals and User Guide Prepared for the US Environmental Protection Agency
626 Office of Research and Development, *Washington, DC*.
- 627 O'Dowd, C. D., M. C. Facchini, F. Cavalli, D. Ceburnis, M. Mircea, S. Decesari, S. Fuzzi, Y.
628 J. Yoon, and J.-P. Putaud (2004), Biogenically driven organic contribution to marine
629 aerosol, *Nature*, *431*(7009), 676-680. <https://doi.org/10.1038/nature02959>.
- 630 O'Dowd, C. D., B. Langmann, S. Varghese, C. Scannell, D. Ceburnis, and M. C. Facchini
631 (2008), A combined organic-inorganic sea-spray source function, *Geophys. Res. Lett.*,
632 *35*(1). <https://doi.org/10.1029/2007GL030331>.
- 633 O'Dowd, C., et al. (2015), Connecting marine productivity to sea-spray via nanoscale
634 biological processes: Phytoplankton Dance or Death Disco?, *Sci Rep*, *5*(1), 14883.



- 635 <https://doi.org/10.1038/srep14883>.
- 636 Park, K.-T., K. Lee, T.-W. Kim, Y. J. Yoon, E.-H. Jang, S. Jang, B.-Y. Lee, and O. Hermansen
637 (2018), Atmospheric DMS in the Arctic Ocean and Its Relation to Phytoplankton Biomass,
638 *Global Biogeochem. Cycles*, 32(3), 351-359. <https://doi.org/10.1002/2017GB005805>.
- 639 Pavuluri, C. M., K. Kawamura, and P. Q. Fu (2015), Atmospheric chemistry of nitrogenous
640 aerosols in northeastern Asia: biological sources and secondary formation, *Atmos.*
641 *Chem. Phys.*, 15(17), 9883-9896. <https://doi.org/10.5194/acp-15-9883-2015>.
- 642 Prather, K. A., et al. (2013), Bringing the ocean into the laboratory to probe the chemical
643 complexity of sea spray aerosol, *Proc. Natl. Acad. Sci. U. S. A.*, 110(19), 7550-7555.
644 <https://doi.org/10.1073/pnas.1300262110>.
- 645 Quinn, P. K., T. S. Bates, K. S. Schulz, D. J. Coffman, A. A. Frossard, L. M. Russell, W. C.
646 Keene, and D. J. Kieber (2014), Contribution of sea surface carbon pool to organic
647 matter enrichment in sea spray aerosol, *Nat. Geosci.*, 7(3), 228-232.
648 <https://doi.org/10.1038/ngeo2092>.
- 649 Rinaldi, M., et al. (2013), Is chlorophyll-a the best surrogate for organic matter enrichment
650 in submicron primary marine aerosol?, *J. Geophys. Res.-Atmos.*, 118(10), 4964-4973.
651 <https://doi.org/10.1002/jgrd.50417>.
- 652 Schiffer, J. M., L. E. Mael, K. A. Prather, R. E. Amaro, and V. H. Grassian (2018), Sea Spray
653 Aerosol: Where Marine Biology Meets Atmospheric Chemistry, *ACS Central Sci.*, 4(12),
654 1617-1623. <https://doi.org/10.1021/acscentsci.8b00674>.
- 655 Sciare, J., O. Favez, R. Sarda-Estève, K. Oikonomou, H. Cachier, and V. Kazan (2009),
656 Long-term observations of carbonaceous aerosols in the Austral Ocean atmosphere:
657 Evidence of a biogenic marine organic source, *J. Geophys. Res.-Atmos.*, 114(D15).
658 <https://doi.org/10.1029/2009JD011998>.
- 659 Shi, J., H. Gao, J. Qi, J. Zhang, and X. Yao (2010), Sources, compositions, and
660 distributions of water-soluble organic nitrogen in aerosols over the China Sea, *J.*
661 *Geophys. Res.-Atmos.*, 115(D17). <https://doi.org/10.1029/2009JD013238>.
- 662 Sun, Y. L., Q. Zhang, J. J. Schwab, W. N. Chen, M. S. Bae, Y. C. Lin, H. M. Hung, and K.
663 L. Demerjian (2011), A case study of aerosol processing and evolution in summer in New
664 York City, *Atmos. Chem. Phys.*, 11(24), 12737-12750. <https://doi.org/10.5194/acp-11-12737-2011>.
- 665
- 666 Tang, J., et al. (2021), Measurement report: Long-emission-wavelength chromophores
667 dominate the light absorption of brown carbon in aerosols over Bangkok: impact from
668 biomass burning, *Atmos. Chem. Phys.*, 21(14), 11337-11352.
669 <https://doi.org/10.5194/acp-21-11337-2021>.
- 670 Tang, J., et al. (2024), Long-Emission-Wavelength Humic-Like Component (L-HULIS) as a
671 Secondary Source Tracer of Brown Carbon in the Atmosphere, *J. Geophys. Res.-Atmos.*,
672 129(5), e2023JD040144. <https://doi.org/10.1029/2023JD040144>.
- 673 Tian, M., et al. (2023), Seasonal source identification and formation processes of marine
674 particulate water soluble organic nitrogen over an offshore island in the East China Sea,
675 *Sci. Total Environ.*, 863, 160895. <https://doi.org/10.1016/j.scitotenv.2022.160895>.
- 676 Tripathee, L., S. Kang, P. Chen, H. Bhattarai, J. Guo, K. L. Shrestha, C. M. Sharma, P.



- 677 Sharma Ghimire, and J. Huang (2021), Water-soluble organic and inorganic nitrogen in
678 ambient aerosols over the Himalayan middle hills: Seasonality, sources, and transport
679 pathways, *Atmos. Res.*, 250. <https://doi.org/10.1016/j.atmosres.2020.105376>.
- 680 Tsagkaraki, M., C. Theodosi, G. Grivas, E. Vargiakaki, J. Sciare, C. Savvides, and N.
681 Mihalopoulos (2021), Spatiotemporal variability and sources of aerosol water-soluble
682 organic nitrogen (WSON), in the Eastern Mediterranean, *Atmos. Environ.*, 246, 118144.
683 <https://doi.org/10.1016/j.atmosenv.2020.118144>.
- 684 Violaki, K., J. Sciare, J. Williams, A. R. Baker, M. Martino, and N. Mihalopoulos (2015),
685 Atmospheric water-soluble organic nitrogen (WSON) over marine environments: a
686 global perspective, *Biogeosciences*, 12(10), 3131-3140. <https://doi.org/10.5194/bg-12-3131-2015>.
- 688 Wang, G. H., et al. (2014), Evolution of aerosol chemistry in Xi'an, inland China, during the
689 dust storm period of 2013 – Part 1: Sources, chemical forms and formation
690 mechanisms of nitrate and sulfate, *Atmos. Chem. Phys.*, 14(21), 11571-11585.
691 <https://doi.org/10.5194/acp-14-11571-2014>.
- 692 Wang, J., et al. (2020), Source apportionment of water-soluble oxidative potential in
693 ambient total suspended particulate from Bangkok: Biomass burning versus fossil fuel
694 combustion, *Atmos. Environ.*, 235, 117624.
695 <https://doi.org/10.1016/j.atmosenv.2020.117624>.
- 696 Wang, X. T., A. L. Cohen, V. Luu, H. Ren, Z. Su, G. H. Haug, and D. M. Sigman (2018),
697 Natural forcing of the North Atlantic nitrogen cycle in the Anthropocene, *Proc. Natl. Acad. Sci. U. S. A.*, 115(42), 10606-10611. <https://doi.org/10.1073/pnas.1801049115>.
- 699 Xie, M., X. Chen, M. D. Hays, M. Lewandowski, J. Offenberg, T. E. Kleindienst, and A. L.
700 Holder (2017), Light Absorption of Secondary Organic Aerosol: Composition and
701 Contribution of Nitroaromatic Compounds, *Environ. Sci. Technol.*, 51(20), 11607-11616.
702 <https://doi.org/10.1021/acs.est.7b03263>.
- 703 Xing, J., J. Song, H. Yuan, Q. Wang, X. Li, N. Li, L. Duan, and B. Qu (2018), Water-soluble
704 nitrogen and phosphorus in aerosols and dry deposition in Jiaozhou Bay, North China:
705 Deposition velocities, origins and biogeochemical implications, *Atmos. Res.*, 207, 90-99.
706 <https://doi.org/10.1016/j.atmosres.2018.03.001>.
- 707 Xu, Y., et al. (2020), Aerosol Liquid Water Promotes the Formation of Water-Soluble
708 Organic Nitrogen in Submicrometer Aerosols in a Suburban Forest, *Environ. Sci. Technol.*, 54(3), 1406-1414. <https://doi.org/10.1021/acs.est.9b05849>.
- 710 Yu, X., et al. (2020), Wet and Dry Nitrogen Depositions in the Pearl River Delta, South
711 China: Observations at Three Typical Sites With an Emphasis on Water-Soluble Organic
712 Nitrogen, *J. Geophys. Res.-Atmos.*, 125(3). <https://doi.org/10.1029/2019jd030983>.
- 713 Yu, X., et al. (2017), Water Soluble Organic Nitrogen (WSON) in Ambient Fine Particles
714 Over a Megacity in South China: Spatiotemporal Variations and Source Apportionment,
715 *J. Geophys. Res.-Atmos.*, 122(23), 13,045-13,060.
716 <https://doi.org/10.1002/2017JD027327>.
- 717 Zamora, L. M., J. M. Prospero, and D. A. Hansell (2011), Organic nitrogen in aerosols and
718 precipitation at Barbados and Miami: Implications regarding sources, transport and



719 deposition to the western subtropical North Atlantic, *J. Geophys. Res.-Atmos.*, 116(D20).
720 <https://doi.org/10.1029/2011JD015660>.
721 Zhao, Y., et al. (2026), Evolution of secondary organic aerosol under extremely high
722 humidity conditions in urban areas of southwestern China: Formation and scavenging,
723 *Atmos. Res.*, 327, 108318. <https://doi.org/10.1016/j.atmosres.2025.108318>.
724 Zhou, S., Y. Chen, A. Paytan, H. Li, F. Wang, Y. Zhu, T. Yang, Y. Zhang, and R. Zhang
725 (2021), Non-Marine Sources Contribute to Aerosol Methanesulfonate Over Coastal Seas,
726 *J. Geophys. Res.-Atmos.*, 126(21), e2021JD034960.
727 <https://doi.org/10.1029/2021JD034960>.
728 Zhou, S., Y. Chen, F. Wang, Y. Bao, X. Ding, and Z. Xu (2023), Assessing the Intensity of
729 Marine Biogenic Influence on the Lower Atmosphere: An Insight into the Distribution of
730 Marine Biogenic Aerosols over the Eastern China Seas, *Environ. Sci. Technol.*, 57(34),
731 12741-12751. <https://doi.org/10.1021/acs.est.3c04382>.
732